

Joint Triplet Autoencoder for Histopathological Colon Cancer Nuclei Retrieval

Satya Rajendra Singh, Shiv Ram Dubey, Shruthi MS, Sairathan Ventrapragada, and Saivamshi Salla Dasharatha

Computer Vision Group, Indian Institute of Information Technology, Sri City, Chittoor, Andhra Pradesh- 517646, India.

satyarajendra.rs@iiits.in, shivram1987@gmail.com, shruthi.msl6@iiits.in, sairathan.v16@iiits.in, saivamshi.s16@iiits.in

Abstract

Deep learning has shown a great improvement in the performance of visual tasks. Image retrieval is the task of extracting the visually similar images from a database for a query image. The feature matching is performed to rank the images. Various hand-designed features have been derived in past to represent the images. Nowadays, the power of deep learning is being utilized for automatic feature learning from data in the field of biomedical image analysis. Autoencoder and Siamese networks are two deep learning models to learn the latent space (i.e., features or embedding). Autoencoder works based on the reconstruction of the image from latent space. Siamese network utilizes the triplets to learn the intra-class similarity and inter-class dissimilarity. Moreover, Autoencoder is unsupervised, whereas Siamese network is supervised. We propose a Joint Triplet Autoencoder Network (JTANet) by facilitating the triplet learning in autoencoder framework. A joint supervised learning for Siamese network and unsupervised learning for Autoencoder is performed. Moreover, the Encoder network of Autoencoder is shared with Siamese network and referred as the Siamcoder network. The features are extracted by using the trained Siamcoder network for retrieval purpose. The experiments are performed over Histopathological Routine Colon Cancer dataset. We have observed the promising performance using the proposed JTANet model against the Autoencoder and Siamese models for colon cancer nuclei retrieval in histopathological images.

1. Introduction

Image retrieval is one of the important problems of computer vision to retrieve the visually matching images from a dataset for a given query image [1]. The ranking of the images is generally carried out by matching the features of a query image with the features of dataset images. Thus, the performance of retrieval depends upon the quality of the features extracted from the images which should be discriminative, robust and low dimensional [2]. Several hand-designed features have been explored in the recent past, such as Local Binary Pattern (LBP) [3], Local Tetra Pattern (LTrP) [4], Multichannel Decoded LBP (mdLBP) [5], Scale Invariant Feature Transform (SIFT) [6], Interleaved Order-based Local Descriptor (IOLD) [7], etc. The hand-designed features have been also explored for biomedical image retrieval such as Local Wavelet Pattern (LWP) [8], Local Mesh Patterns (LMeP) [9], Local Bit-plane Decoded Pattern (LBDP) [10], Local Ternary Co-occurrence Patterns (LTCoP) [11], Local Diagonal Extrema Pattern (LDEP) [12], etc.

In the recent past, a paradigm shift has been observed from the hand-designed feature extraction to the data driven feature learning. Thanks to the recently emerged Deep learning [13] which facilitates the feature learning automatically from the data. Convolutional Neural Network (CNN) is a type of Neural Network designed to deal with the image and video data. AlexNet was the first CNN model developed for image classification problem in 2012. The imagenet visual recognition challenge was won by AlexNet in 2012 with a great margin as

compared to the best performing hand-designed features. Since 2012, various CNN models have been proposed for different applications such as image classification [14], object detection [15], image segmentation [16], face recognition/retrieval [17], [18], face anti-spoofing [19], [20], facial micro-expression recognition [21], [22], hyperspectral image classification [23], [24], image-to-image translation [25], [26], [27], and many more.

Sirinukunwattana et al. have introduced a Spatially Constrained Convolutional Neural Network (SC-CNN) for histopathological routine colon cancer (RCC) nuclei detection and recognition [28]. Moreover, they have also collected the RCC nuclei dataset which is used in this paper for the experiments in retrieval framework. Recently, Basha et al. have developed a RCCNet CNN model having less number of parameters for the classification of RCC Nuclei patches [29]. Rajpurkar et al. have developed a ChexNet CNN model over chest X-rays data for pneumonia detection [30]. Wang et al. have proposed a Text-image embedding network (TieNet) for recognising the thorax disease in chest X-rays [31]. Recently, the deep learning based methods are also proposed for biomedical image retrieval [32], [33], [34]. Gu and Yang have used the dense connection for multi-magnification hashing applied over histopathological images [35]. A very recently, Sun et al. have used the adversarial learning for lesion detection [36]. Li et al. have developed a dual-channel deep neural network to identify the antiviral peptides [37].

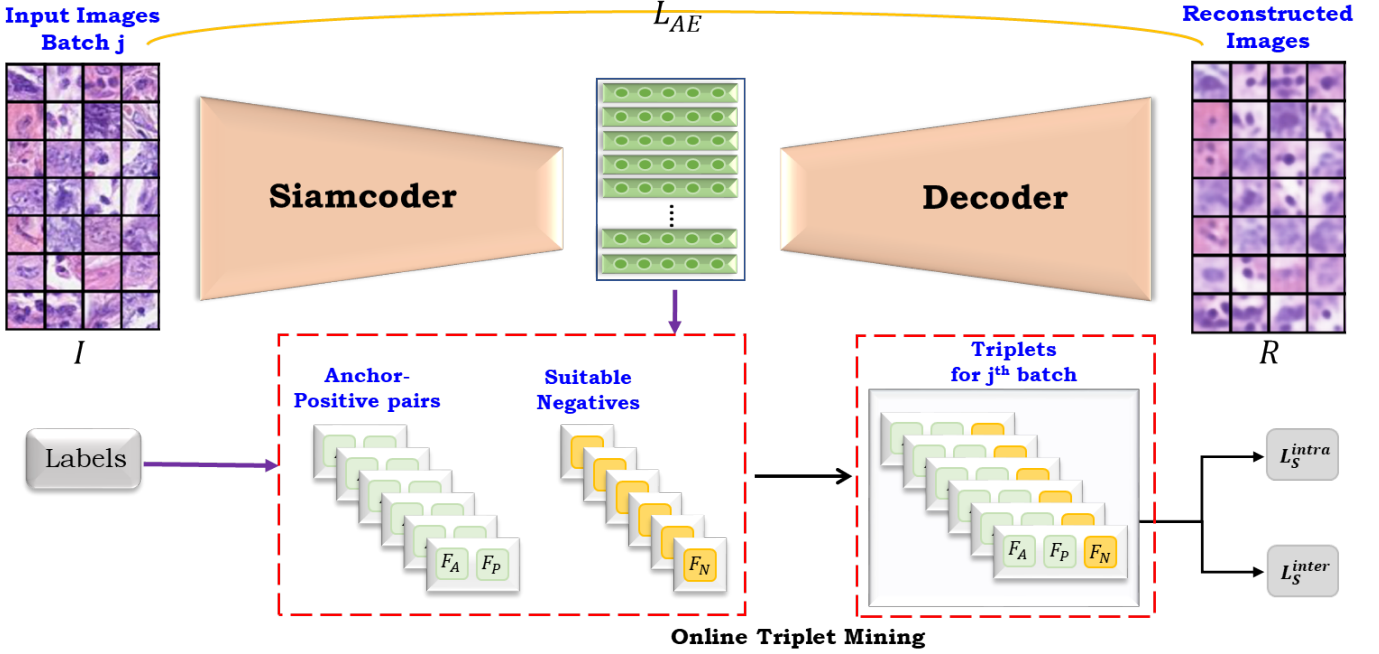


Figure 1: The proposed Joint Triplet Autoencoder Network (JTANet) model for feature learning using Autoencoder and Siamese networks in joint fashion using triplets generated through online triplet mining.

Autoencoder is one of the type of Neural Network which tries to learn the latent space through reconstruction process [38]. Basically, first the input image is projected to a latent space (i.e., feature space) using an Encoder network and then it is reconstructed from that latent space using a Decoder network. The loss between the original image and the reconstructed image is minimized using Stochastic Gradient Descent (SGD) Optimization to learn the Encoder and the Decoder networks. Krizhevsky and Hinton have used a deep autoencoder for content-based image retrieval [39]. Zhang et al. have used the stack of sparse autoencoder and fused its features for histopathology image analysis [40]. Leng et al. have utilised the autoencoder with CNN for 3D object retrieval [41]. Zhu et al. have also exploited the features learnt through autoencoder for 3D shape retrieval [42]. The autoencoder has been also used in medical area such as autoencoder-based hybrid CNN-LSTM model for COVID-19 severity prediction [43], detection of interacting protein pairs via ensemble of autoencoder and LightGBM [44], Convolutional Autoencoders to study the Alzheimer’s Disease [45] and Optimizing autoencoders based network to analyze health data [46]. The major drawback of such models is that they are completely unsupervised and not able to learn the discriminative features.

Siamese network is a supervised learning framework to learn the features from triplets [47]. A triplet contains three images with two from same class and one from different class. Siamese network tries to minimize the intra-class distance and maximize the inter-class distance. A pair-wise cosine loss and quantization loss is used by Cao et al. to learn the feature for image retrieval [48]. Further, they have introduced a HashNet model for retrieval [49]. A triplet ranking loss is used by Yao et al. for

semantic preserving image retrieval [50]. A deep supervised hashing is developed by Liu et al. by utilizing the discriminative and binarization loss [51]. Yang et al. have introduced a semantic preserving deep hash (SSDH) code using CNN for image retrieval [52]. Li et al. have developed the deep supervised discrete hashing method to learn the binary features [53]. Zhang et al. have introduced a semi-supervised hashing model by incorporating the supervised classification in semi-supervised hash learning framework [54]. An asymmetric deep supervised hashing is proposed by Jiang and Li by incorporating asymmetric pairwise loss [55]. Recently, Wu et al. have proposed a deep incremental hashing network to learn the hash codes of new images without changing the hash code of existing images [56]. Siamese neural networks are also used for spinal metastasis detection [57]. The major problem with Siamese network is that the learnt feature is very specific to that dataset. Moreover, it is derived only from one-way mapping (i.e., no mapping from feature to image), thus the discriminative ability might be compromised over the unseen data.

It is observed from the literature that Siamese networks and Autoencoder networks have its limitation in terms of the generalizability and discriminativeness. We propose a Joint triplet Autoencoder Network (JTANet) to learn the Encoder network of Autoencoder as a Siamese network which is termed as a Siamcoder network in this paper. Basically the triplets are used for learning of Siamcoder network in a joint fashion. The main contributions of this paper are as follows:

- A semi-supervised Joint Triplet Autoencoder Network (JTANet) is proposed by utilizing the Siamese and Autoencoder networks.
- A Siamcoder network is used as a common CNN for

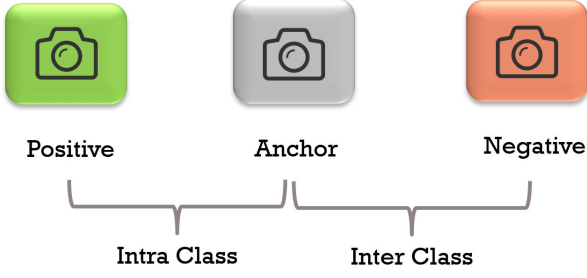


Figure 2: The triplet depicting the intra-class and inter-class samples.

Siamese network as well as Encoder network of Autoencoder.

- A joint training is performed for supervised Siamese network and unsupervised Autoencoder network.
- The latent space output of Siamcoder network is used as the feature vector/embedding for the retrieval purpose.
- The joint training enhances the generalizability and discriminativeness of the latent space.
- The histopathological colon cancer nuclei retrieval experiments are performed by using the features derived from the learnt Siamcoder network of the JTANet model.
- The effect of different losses is analyzed through experiments.

The organization of the paper is as follows. Section II describes the proposed JTANet model; Section III presents the histopathological colon cancer nuclei retrieval framework using JTANet model; Section IV describes the experimental settings; Section V illustrates the experimental results and analysis; and finally, Section VI concludes the paper.

2. Proposed Joint Triplet Autoencoder Network

A Joint Triplet Autoencoder Network (JTANet) is proposed in this paper which combines the power of Siamese and Autoencoder networks. The proposed JTANet model is illustrated in Fig. 1. A Siamcoder network (SCN) (basically the encoder network of Autoencoder) is used to transform an image patch (I) into the feature/latent space/embedding (F). Note that the Siamcoder network is shared between the Siamese network (SN) and Autoencoder network (AN). The Siamcoder network is a Convolutional Neural Network (CNN) having different layers such as convolution, batch normalization, activation function, and max pooling. Basically, the non-linear transformation function of Siamcoder network is denoted as $f_{SCN} : \mathbb{R}^{m \times m \times 3} \rightarrow \mathbb{R}^{dim}$ which converts the two-dimensional data of size $m \times m$ having three channels into an one-dimensional feature vector of size dim . Thus, f_{SCN} can be seen as a hierarchy of some linear and non-linear functions. The Decoder network (DN) of Autoencoder is an Up-Convolutional Neural Network to reconstruct the output image from the latent space which

is corresponding to the original image. It is also a non-linear function having different layers such as transpose-convolution, batch normalization, activation function, and upsampling. The transformation function for the Decoder network is denoted as $f_{DN} : \mathbb{R}^{dim} \rightarrow \mathbb{R}^{m \times m \times 3}$ which transforms the one-dimensional feature F of size dim into an image patch R of size $m \times m$ with three channels. Note that R is the reconstructed image w.r.t. the original image I .

Consider $\{I_A, I_P, I_N\}$ as a triplet of patches with $C_{I_A} = C_{I_P}$ and $C_{I_A} \neq C_{I_N}$ where C_{I_k} represents the class label for image patch I_k for $k \in \{A, P, N\}$. The image patches I_A , I_P , and I_N are referred as the Anchor, Positive and Negative samples, respectively. A pictorial representation of triplet is shown in Fig. 2. The proposed JTANet network generates the triplets of image patches for a batch of input from its latent space using online triplet mining as portrayed in Fig. 1 at the training time. However, it only needs a single image at test time to extract the features. Thus, the features used by online triplet mining for a batch of images are computed by the same Siamcoder network. The feature vectors are normalized before online triplet mining.

2.1. Objective Function

Three losses, namely Autoencoder loss, Siamese loss and Feature Regularization loss are used as the objective function to train the JTANet model. Mathematically, the objective function of the proposed JTANet model is given as,

$$L_{JTA} = \lambda_{AE}L_{AE} + \lambda_{SM}L_{SM} + \lambda_{FR}L_{FR} \quad (1)$$

where L_{JTA} is the final loss function, L_{AE} is the Autoencoder loss, L_{SM} is the Siamese loss, L_{FR} is the Feature Regularization loss and $\{\lambda_{AE}, \lambda_{SM}, \lambda_{FR}\}$ are the hyper-parameters as the weights for the Autoencoder, Siamese, and Feature Regularization losses, respectively.

2.1.1. Autoencoder Loss

The Autoencoder loss (L_{AE}) is computed between the original images I_k and its corresponding regenerated images R_k for a batch of input. The purpose of Autoencoder loss is to make sure that the relevant features are being learnt by Siamcoder network. It is ensured by reconstructing the image from feature/latent space. Thus, it makes sure that Siamcoder network should not learn the random features. Mathematically, L_{AE} is given as,

$$L_{AE} = \sum_{i=1}^B L_{AE_i} \quad (2)$$

where B is the batch size (i.e., the number of samples in a batch) and L_{AE_i} is the Autoencoder loss between the i^{th} input image patch I_i and its corresponding reconstructed image patch R_i for a batch. The L_{AE_i} is computed as the mean square error (MSE) between I_i and R_i and given as,

$$\begin{aligned} L_{AE_i} &= \|I_i - R_i\|_{avg}^2 \\ &= \frac{1}{m \times m \times 3} \sum_{u=1}^m \sum_{v=1}^m \sum_{c=1}^3 (I_i(u, v, c) - R_i(u, v, c))^2 \end{aligned} \quad (3)$$

where $I_i(u, v, c)$ and $R_i(u, v, c)$ denote the values in the image patches I_i and R_i , respectively at image co-ordinate (u, v) in c^{th} channel and $\|\cdot\|_{avg}^2$ represents the mean square error (MSE).

2.1.2. Siamese Loss

The online triplet mining uses the features derived from Siamcoder network to generate the triplets of the Anchor, Positive and Negative samples. Consider, $\{F_A, F_P, F_N\}$ as the Anchor, Positive and Negative triplets of Siamcoder network generated features corresponding to the Anchor, Positive and Negative image patch triplet $\{I_A, I_P, I_N\}$, respectively. The Siamese loss (L_{SM}) is computed by using the $\{F_A, F_P, F_N\}$ features corresponding to the Anchor, Positive and Negative samples. The purpose of Siamese loss is to decrease the distance between the features of Anchor and Positive samples and to increase the distance between the features of Anchor and Negative samples. By doing so, it forces the Siamcoder network to learn the class specific features such that the features for samples of same class are closer to each other and the features for samples of different class are apart from each other. The L_{SM} is given as,

$$L_{SM} = \begin{cases} 0 & L_S \leq 0 \\ L_S & \text{Otherwise} \end{cases} \quad (4)$$

where L_S is defined as,

$$L_S = L_S^{intra} - L_S^{inter} + \lambda_m \quad (5)$$

where L_S is the Siamese loss, L_S^{intra} is the Siamese intra-class similarity loss, L_S^{inter} is the Siamese inter-class similarity loss, and λ_m is a margin hyper-parameter. The Siamese intra-class similarity loss is computed between the features of the samples of the same class (i.e., F_A and F_P). Similarly, the Siamese inter-class similarity loss is computed between the features of the samples of the different classes (i.e., F_A and F_N). These losses are computed as,

$$L_S^{intra} = \sum_i^{nb} \|F_A^i - F_P^i\|^2 = \sum_i^{nb} \sum_{v=1}^{dim} (F_A^i(v) - F_P^i(v))^2 \quad (6)$$

and

$$L_S^{inter} = \sum_i^{nb} \|F_A^i - F_N^i\|^2 = \sum_i^{nb} \sum_{v=1}^{dim} (F_A^i(v) - F_N^i(v))^2 \quad (7)$$

where F_A^i , F_P^i , and F_N^i are the feature vectors of size dim derived using Siamcoder network for i^{th} triplet having Anchor (I_A^i), Positive (I_P^i), and Negative (I_N^i) image patches, respectively, nb is the number of triplets generated by online triplet mining for a batch of input and $\|\cdot\|^2$ represents the sum of square distances (SSD).

2.1.3. Feature Regularization Loss

The Feature Regularization loss (L_{FR}) is computed from the Siamcoder network's output features (F_i for $1 \leq i \leq B$). The purpose of Feature Regularization loss is to increase the generalization

ability of features being produced by the the Siamcoder network. It is computed as,

$$L_{FR} = \sum_{i=1}^B L_{FR}^i \quad (8)$$

where L_{FR}^i for $1 \leq i \leq B$ is the Feature Regularization loss over the feature vector F_i and defined as,

$$L_{FR}^i = \|F_i\|_{norm}^2 = \sum_{v=1}^{dim} (F_i(v))^2 \quad (9)$$

by calculating the L_2 -Norm of feature vector F_i for $i \in [1, B]$.

We use Stochastic Gradient Descent (SGD) based optimization techniques called as Adam to train the Siamcoder and Decoder networks of the proposed JTANet model. The weights of any network in deep learning are generally trained by updating it during backpropagation of training using SGD based update rules [58], [59].

3. Routine Colon Cancer Nuclei Retrieval using Proposed JTANet Model

The proposed JTANet model is trained using the Routine Colon Cancer (RCC) Nuclei triplets. The training is performed for Siamcoder and Decoder networks in joint fashion using Autoencoder, Siamese, and Regularization losses. Once the JTANet model is trained, only Siamcoder network is required to extract the features from any image patch as depicted in Fig. 3. A training feature database is created as follows,

$$F_{i,C_i}^{train} |_{i=1,2,\dots,N^{train}} = f_{SCN}(I_{i,C_i}^{train}) \quad (10)$$

where N^{train} is the total number of images in the training set, I_{i,C_i}^{train} is the i^{th} image in the training set having C_i as the class label, f_{SCN} is the Siamcoder network function to transform an image patch into a feature vector, and F_{i,C_i}^{train} is the extracted features for image patch I_{i,C_i}^{train} . Consider I^q as a query image patch for which we want to retrieve the best δ number of images from training set. The features F_q are also extracted for input query I^q using the same trained Siamcoder network to facilitate the feature matching as,

$$F^q = f_{SCN}(I^q). \quad (11)$$

Note that for the experimentation purpose, the query image patch I^q is taken from the test set of the Routine Colon Cancer Nuclei database. Thus, $q = 1, 2, 3, \dots, N^{test}$ where N^{test} is the number of images in the test set. The distance between features of query image F^q and training images F_{i,C_i}^{train} for $i = 1, 2, \dots, N^{train}$ is computed to retrieve the best δ images from training set based on the distance ranking in increasing order as illustrated in Fig. 3. The Euclidean distance is computed between the features as follows:

$$dis(F^q, F_{i,C_i}^{train}) = \left(\sum_{z=1}^{dim} (F^q(z) - F_{i,C_i}^{train}(z))^2 \right)^{0.5}. \quad (12)$$

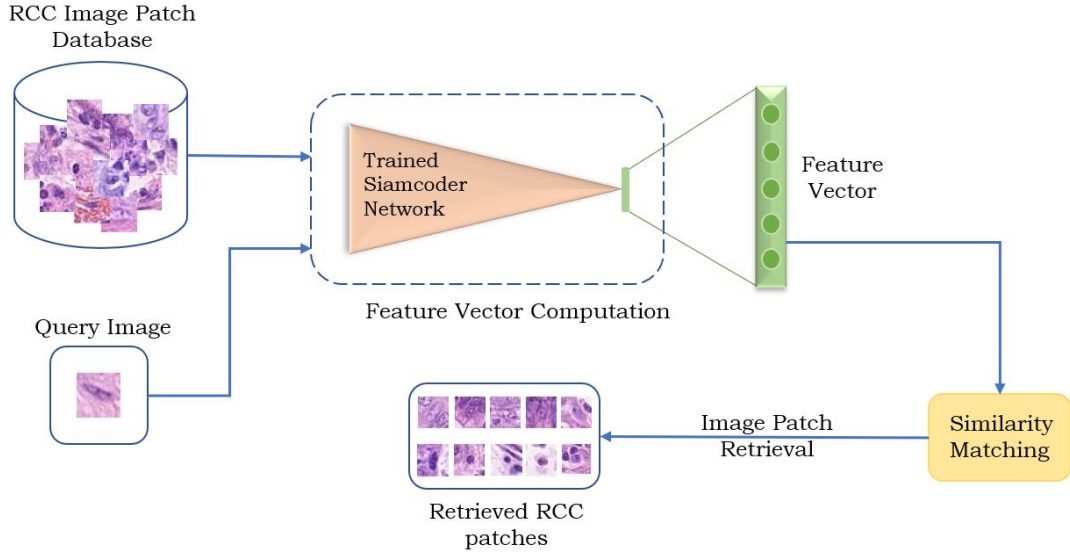


Figure 3: The image retrieval framework in Routine Colon Cancer (RCC) image patch database using the proposed trained Siamcoder network.

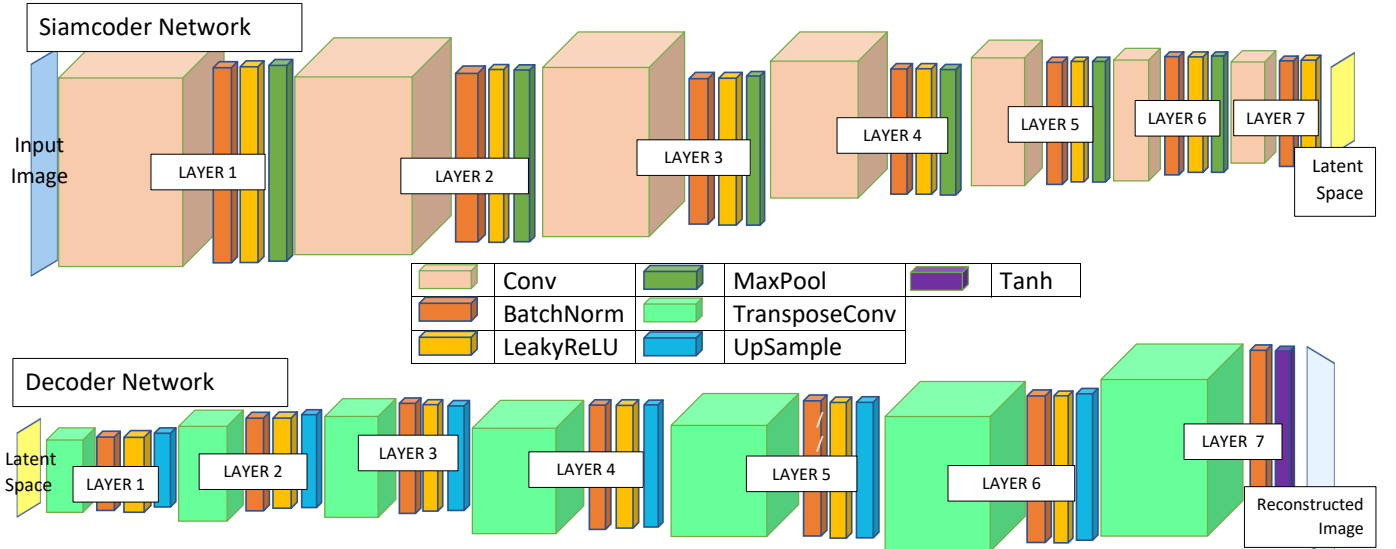


Figure 4: The Siamcoder and Decoder architectures of the proposed JTANet model.

The performance of the model is computed by considering each image patch in test as the query image one by one. Consider I_{j,C_j}^{test} as the j^{th} sample in the test set as the query patch q from C_j^{th} class where N^{test} is the total number of RCC image patches in the test set. The feature extracted using trained Siamcoder network for test image patch I_{j,C_j}^{test} is F_{j,C_j}^{test} . The mean precision is computed as,

$$Pr = \frac{\sum_{j=1}^{N^{test}} Pr_j}{N^{test}} \quad (13)$$

where Pr_j is the precision when j^{th} test sample is considered as

the query and computed as,

$$Pr_j = 100 \times \frac{\#CR_j}{\#TR_j} \quad (14)$$

where $\#CR_j$ and $\#TR_j$ are the number of correctly retrieved and total retrieved images for a query.

4. Experimental Settings

This section is devoted for the architecture details, dataset description, triplet generation and hyper-parameter settings.

Table 1: Layer wise details of the proposed JTANet architecture. Each Conv and ConvTranspose layer uses 3x3 filters without bias with stride 1 and padding 1, each LeakyReLU layer uses 0.2 leaky factor, each MaxPool layer uses 2x2 kernel with stride 2 and each UpSample layer uses scaling factor 2 with bilinear upsampling strategy. The embedding length is represented by EL. The Tanh is the activation function in the last layer of the decoder network.

Layer	SIAMCODER Network			DECODER Network		
	Filter	Input Dimension	Output Dimension	Filter	Input Dimension	Output Dimension
1	Conv	64x64x3	64x64x64	ConvTranspose	1x1xEL	1x1x1024
	BatchNorm, LeakyReLU	64x64x64	64x64x64	BatchNorm, LeakyReLU	1x1x1024	1x1x1024
	MaxPool	64x64x64	32x32x64	UpSample	1x1x1024	2x2x1024
2	Conv	32x32x64	32x32x128	ConvTranspose	2x2x1024	2x2x1024
	BatchNorm, LeakyReLU	32x32x128	32x32x128	BatchNorm, LeakyReLU	2x2x1024	2x2x1024
	MaxPool	32x32x128	16x16x128	UpSample	2x2x1024	4x4x1024
3	Conv	16x16x128	16x16x256	ConvTranspose	4x4x1024	4x4x512
	BatchNorm, LeakyReLU	16x16x256	16x16x256	BatchNorm, LeakyReLU	4x4x512	4x4x512
	MaxPool	16x16x256	8x8x256	UpSample	4x4x512	8x8x512
4	Conv	8x8x256	8x8x512	ConvTranspose	8x8x512	8x8x256
	BatchNorm, LeakyReLU	8x8x512	8x8x512	BatchNorm, LeakyReLU	8x8x256	8x8x256
	MaxPool	8x8x512	4x4x512	UpSample	8x8x256	16x16x256
5	Conv	4x4x512	4x4x1024	ConvTranspose	16x16x256	16x16x128
	BatchNorm, LeakyReLU	4x4x1024	4x4x1024	BatchNorm, LeakyReLU	16x16x128	16x16x128
	MaxPool	4x4x1024	2x2x1024	UpSample	16x16x128	32x32x128
6	Conv	2x2x1024	2x2x1024	ConvTranspose	32x32x128	32x32x64
	BatchNorm, LeakyReLU	2x2x1024	2x2x1024	BatchNorm, LeakyReLU	32x32x64	32x32x64
	MaxPool	2x2x1024	1x1x1024	UpSample	32x32x64	64x64x64
7	Conv	1x1x1024	1x1xEL	ConvTranspose	64x64x64	64x64x3
	BatchNorm, LeakyReLU	1x1xEL	1x1xEL	BatchNorm, Tanh	64x64x3	64x64x3

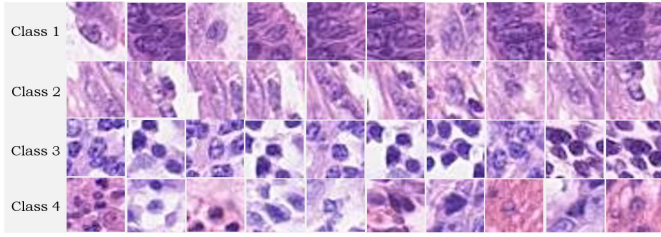


Figure 5: Sample image patches from Histopathological Routine Colon Cancer (RCC) Nuclei Cell dataset.

4.1. Architecture for Siamcoder and Decoder Networks

The proposed model uses Siamcoder and Decoder networks for feature extraction and image patch reconstruction, respectively as depicted in Fig. 4. The Siamcoder network consists of seven convolution layers. The Decoder network also consists of seven deconvolutional layers. The layer-wise details of the proposed JTANet model is summarized in Table 1.

4.2. Routine Colon Cancer Dataset

A CRCHistoPhenotypes - Labeled Routine Colon Cancer (RCC) Cell Nuclei Dataset¹ is used in this paper for the experiments [28]. This dataset contains 100 H&E stained histology images of colorectal adenocarcinomas. The co-ordinates of 22,444 RCC nuclei is also provided with this dataset along with its associated labels. Basically, this RCC dataset has 4 classes which are named as, epithelial, fibroblast, inflammatory and others. We use the co-ordinates of nuclei cells to extract the 32 × 32 patches around the cells. The image patches

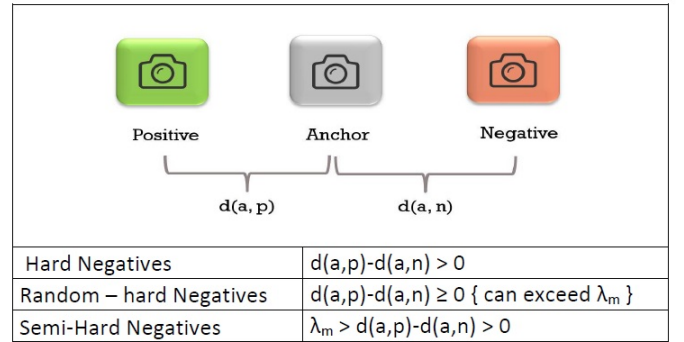


Figure 6: Different strategies used for the negatives selection of triplets.

are distributed unevenly among four classes (i.e., epithelial-7,722 patches, fibroblast-5,712 patches, inflammatory-6,971 patches, others-2,039 patches). The dimension of the RCC image patches is 32 × 32 having 3 channels. The sample image patches of RCC dataset is shown in Fig. 5. The dataset is split into train and test sets having 20,444 and 2,000 image patches, respectively.

4.3. Triplet Generation

Online triplet mining [60] is used in this work to generate the triplets. Only training set is used to generate the triplets as it is needed only at training time. First, the Anchor-Positive pairs are generated using the distance matrix computed from the embeddings extracted by the siamcoder network. Next, a suitable negative sample for each Anchor-Positive pair is selected to form the triplet. The negative sample is taken from any other class than anchor class using the negative selection function. A triplet score is passed as the input to the

¹<https://warwick.ac.uk/fac/sci/dcs/research/tia/data/crchistolabelednuclei/>

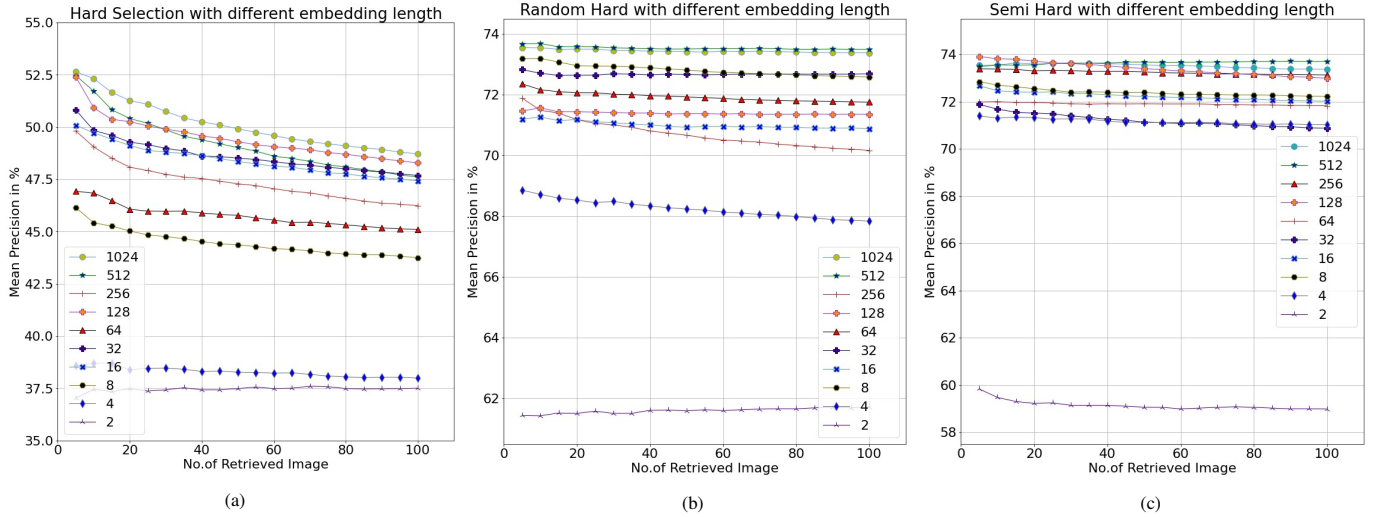


Figure 7: The mean precision computed using the proposed JTANet model for different no. of retrieved images using (a) Hard, (b) Random Hard, and (c) Semi Hard negative selection strategies of triplet generation.

negative selection function. The triplet score is computed as $\max(d(A, P) - d(A, N) + \lambda_m, 0)$ where d is the distance function, A , P , and N are the Anchor, Positive, and Negative samples of any triplet, and the margin λ_m is a hyper-parameter. We use three types of negative sample selection approaches as shown in Fig 6 and described as follows:

- **Hard Negative:** The difference between the distances should be greater than zero. The negatives sorted in descending order of the score values and the negative with largest score value is selected for an anchor-positive pair.
- **Semi-hard Negative:** The difference between the distances should be greater than zero and at the same time it should not exceed the margin. All such negatives satisfying the condition are considered and one of them is selected as the suitable negative for a given anchor-positive pair.
- **Random-hard Negative:** A combination of both hard and semi-hard triplets is considered. The negatives are randomly selected which satisfy a common condition that the difference in the distances should be greater than zero.

4.4. Hyper-parameter Settings

The experiments are conducted using the PyTorch framework. The Adam optimiser is used with 0.001 learning rate for 50 epochs. The batch size is set to 256. The input patch dimension is resized to $64 \times 64 \times 3$. In random-hard and semi-hard negative selections, the margin threshold value (λ_m) used is 0.5. The default weight factors/coefficients for all the loss functions are used as 1 until or otherwise specified.

5. Experimental Results and Analysis

In this section, the performance of the proposed JTANet model is reported and analyzed for different settings under retrieval framework. First, we report the experimental results for

Hard, Random Hard and Semi Hard triplet selection strategies. Then, we conduct the convergence analysis and finally, the loss weight coefficient analysis is done.

5.1. Results using Different Embedding Lengths

The experimental results in terms of the mean retrieval precision is demonstrated in Fig. 7. The mean precision values are plotted against the number of images retrieved from 5 to 100. The embedding lengths (i.e., the latent space feature dimension) used are 2, 4, 8, 16, 32, 64, 128, 256, 512 and 1024. The plots in Fig. 7a, Fig. 7b, and Fig. 7c correspond to the Hard, Random Hard, and Semi Hard negative selection strategies of triplet generation, respectively. Generally, the mean precision decreases with increase in the number of retrieved images.

The best performance is achieved for 1024 embedding length in case of Hard selection. Whereas, the best performance is observed for 512 embedding length in case of Random Hard and Semi Hard selections. The possible reason of such behaviour is associated with the difficulty of the triplets which is more in case of Hard selection based strategy. It is also noticed that the mean precision is lowest for embedding length 2 across all the plots. Moreover, the performance is lower with smaller embedding lengths in most of the cases due to the limited discriminative power of less features. The mean precision for Random Hard and Semi Hard strategies is better than Hard strategy. The mean precision values for 5 number of retrieved images using the proposed JTANet method is also reported in Table 2 using Hard, Random Hard and Semi Hard strategies. It shows the suitability of the proposed model for routine colon cancer patch retrieval task.

5.2. The Convergence Analysis

In order to understand the training behaviour of the proposed JTANet model, the convergence analysis is done in this paper. Fig. 8 shows the loss values for autoencoder loss, siamese loss, feature regularization loss, and total loss in terms of the number

Table 2: The mean precision obtained using the proposed JTANet method for different embedding length for 5 no. of retrieved images.

Embedding length	HARD	RANDOM HARD	SEMI HARD
1024	52.64	73.56	73.52
512	52.46	73.67	73.47
256	49.82	71.88	73.39
128	52.40	71.46	73.90
64	46.93	72.36	71.98
32	50.82	72.82	71.87
16	50.08	71.20	72.66
8	46.15	73.18	72.83
4	38.58	68.85	71.38
2	37.03	61.43	59.82

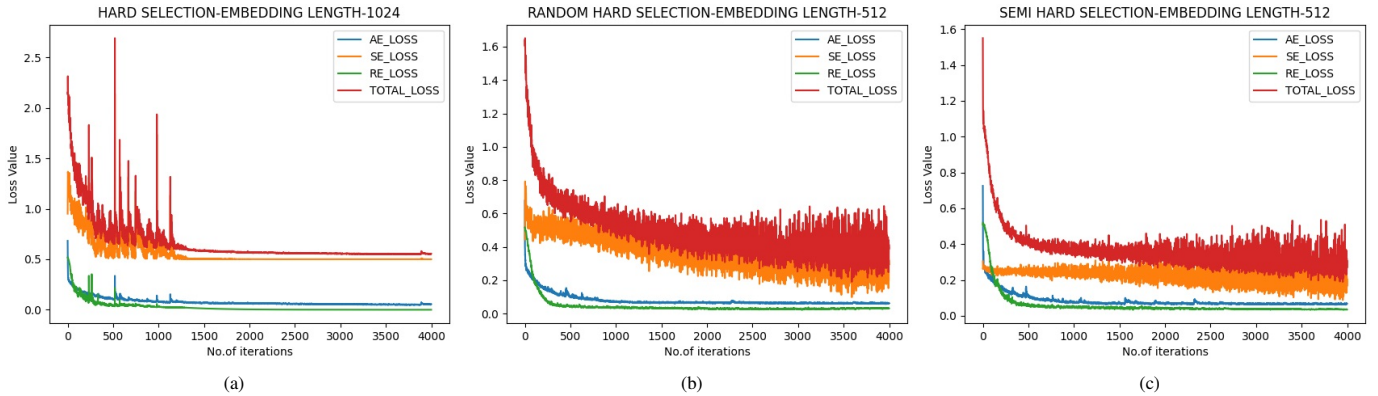


Figure 8: The loss values using the proposed JTANet model w.r.t. the training iterations using (a) Hard, (b) Random Hard, and (c) Semi Hard negative selection strategies of triplet generation. Here, AE_LOSS, SE_LOSS, RE_LOSS, and TOTAL_LOSS refer to autoencoder loss, siamese loss, feature regularization loss and total loss, respectively.

of the training iterations. The loss curves in Fig. 8a, Fig. 8b, and Fig. 8c correspond to the Hard, Random Hard, and Semi Hard strategies, respectively. The same unit weights are used for each loss to compute the total loss in this experiment. The graph is plotted for Hard negative selection of triplet with the feature length 1024. Whereas, the feature length 512 is used for Random Hard and Semi Hard negative selection of triplet strategies. It is observed from this plot that the training has been converged well w.r.t. all the loss functions. Moreover, the siamese loss dominates over other two losses. The fluctuations in the siamese loss of Random Hard as well as Semi Hard are due to the random triplets being generated in different iterations. Whereas, no randomness is present in Hard selection strategy, thus smoother loss curves have been observed. The autoencoder loss and feature regularization loss are converged within 1000 iterations in all the cases. The siamese loss also converges in reasonable number of epochs in all the cases. From this result, it is evident that the proposed JTANet model shows the faster convergence in training.

5.3. The Loss Weight Coefficient Analysis

The high precision using the proposed JTANet model is observed due to the different losses used, such as autoencoder loss, siamese loss and feature regularization loss. The total loss is computed as the weighted combination of above mentioned

three losses. In earlier experiments, all the weight coefficients are set as 1. In this experiment, the performance comparison is done by varying the weight coefficients for different losses in order to compute the total loss. The mean precision (%) using the proposed JTANet model by varying the weight settings of different losses for 5 number of retrieved images is reported in Table 3. The feature lengths used for Hard, Random Hard and Semi Hard triplet selection strategies are 1024, 512 and 512, respectively in this experiment.

The different weight coefficient combinations for Autoencoder Loss (AE), siamese loss (SM) and feature regularization loss (FR) (i.e., AE:SM:FR) are 1:1:1, 5:1:1, 1:5:1, 1:1:5, 10:1:1, 1:10:1, 1:1:10, 0:1:1, 1:0:1 and 1:1:0, respectively. From Table. 3, we notice that when the autoencoder loss is missing (i.e., the weight values are 0:1:1), the mean precision is best for Hard and Random Hard triplets. However, the autoencoder loss is influential with Semi Hard triplets. When the weight values are 1:5:1 (i.e., more weight given to siamese loss), the mean precision is best for Semi-Hard triplets. The biased weighted highest mean precision is improved as compared to the ideal weighted (1:1:1) mean precision by 11.65%, 0.60%, and 0.97% for Hard, Random Hard and Semi Hard selection strategies, respectively. It is also observed that very high weight for siamese loss (i.e., 1:10:1 setting) lowers the performance for Hard selection. Whereas, it is evident from 1:0:1 setting that the siamese

Table 3: The mean precision in % using the proposed JTANet model by varying the weight coefficient settings of different losses for 5 number of retrieved images. The embedding lengths used for Hard, Random-Hard and Semi-Hard triplet strategies are 1024, 512 and 512, respectively.

AE:SM:FR	Hard-1024	Random-Hard-512	Semi-Hard-512
1:1:1	52.64	73.67	73.47
5:1:1	50.41	72.21	73.96
1:5:1	47.90	73.50	74.18
1:1:5	48.24	72.03	72.85
10:1:1	51.14	72.25	72.36
1:10:1	43.65	73.43	72.86
1:1:10	48.10	73.13	73.27
0:1:1	58.77	74.11	73.60
1:0:1	50.76	52.12	44.24
1:1:0	50.09	70.78	72.23

loss is the most important loss for Random Hard and Semi Hard triplet selection strategies. We can say from this experiment that following is the relevancy of different losses: siamese loss > feature regularization loss > autoencoder loss in the proposed JTANet model for routine colon cancer patch retrieval.

6. Conclusion

This paper proposes a joint triplet autoencoder network (JTANet) for histopathological colon cancer nuclei retrieval. The proposed JTANet is a joint venture of the autoencoder and siamese networks. The encoder network of autoencoder is shared with the siamese network. The main aim of the proposed model is to learn more discriminative, robust and efficient feature embeddings for the retrieval task. In order to achieve it, three losses, namely autoencoder loss, siamese loss and feature regularization loss are used. The siamese loss is computed from the triplets which is generated from the embeddings itself using Hard, Random Hard and Semi Hard strategies. The image retrieval experiments are conducted over histopathological colon cancer nuclei dataset. The experimental results suggest that the Semi Hard triplet selection method with 512 embedding length is the most suitable for JTANet with 1:5:1 weighting between autoencoder, siamese and regularization losses. It is also observed that the proposed JTANet model exhibits the faster convergence property. The autoencoder loss is not important with Hard triplet selection strategy. It is also noticed that the siamese loss dominates over other losses in Random Hard and Semi Hard strategies. The experimental results confirm the suitability of the proposed JTANet model for RCC patch retrieval.

7. Acknowledgment

This research is funded by Science and Engineering Research Board (SERB), Govt. of India through Project Sanction Number ECR/2017/000082. The authors would like to thank NVIDIA Corporation for the support of 2 GeForce Titan X Pascal GPUs.

References

- [1] Y. Liu, D. Zhang, G. Lu, W.-Y. Ma, A survey of content-based image retrieval with high-level semantics, *Pattern recognition* 40 (1) (2007) 262–282. [1](#)
- [2] M. Pietikäinen, A. Hadid, G. Zhao, T. Ahonen, *Computer vision using local binary patterns*, Vol. 40, Springer Science & Business Media, 2011. [1](#)
- [3] T. Ahonen, A. Hadid, M. Pietikainen, Face description with local binary patterns: Application to face recognition, *IEEE Transactions on Pattern Analysis & Machine Intelligence* (12) (2006) 2037–2041. [1](#)
- [4] S. Murala, R. Maheshwari, R. Balasubramanian, Local tetra patterns: a new feature descriptor for content-based image retrieval, *IEEE transactions on image processing* 21 (5) (2012) 2874–2886. [1](#)
- [5] S. R. Dubey, S. K. Singh, R. K. Singh, Multichannel decoded local binary patterns for content-based image retrieval, *IEEE transactions on image processing* 25 (9) (2016) 4018–4032. [1](#)
- [6] D. G. Lowe, Distinctive image features from scale-invariant keypoints, *International journal of computer vision* 60 (2) (2004) 91–110. [1](#)
- [7] S. R. Dubey, S. K. Singh, R. K. Singh, Rotation and illumination invariant interleaved intensity order-based local descriptor, *IEEE Transactions on Image Processing* 23 (12) (2014) 5323–5333. [1](#)
- [8] S. R. Dubey, S. K. Singh, R. K. Singh, Local wavelet pattern: a new feature descriptor for image retrieval in medical ct databases, *IEEE Transactions on Image Processing* 24 (12) (2015) 5892–5903. [1](#)
- [9] S. Murala, Q. J. Wu, Local mesh patterns versus local binary patterns: biomedical image indexing and retrieval, *IEEE journal of biomedical and health informatics* 18 (3) (2013) 929–938. [1](#)
- [10] S. R. Dubey, S. K. Singh, R. K. Singh, Local bit-plane decoded pattern: a novel feature descriptor for biomedical image retrieval, *IEEE Journal of Biomedical and Health Informatics* 20 (4) (2015) 1139–1147. [1](#)
- [11] S. Murala, Q. J. Wu, Local ternary co-occurrence patterns: a new feature descriptor for mri and ct image retrieval, *Neurocomputing* 119 (2013) 399–412. [1](#)
- [12] S. R. Dubey, S. K. Singh, R. K. Singh, Local diagonal extrema pattern: a new and efficient feature descriptor for ct image retrieval, *IEEE Signal Processing Letters* 22 (9) (2015) 1215–1219. [1](#)
- [13] Y. LeCun, Y. Bengio, G. Hinton, Deep learning, *nature* 521 (7553) (2015) 436–444. [1](#)
- [14] K. He, X. Zhang, S. Ren, J. Sun, Deep residual learning for image recognition, in: *Proceedings of the IEEE conference on computer vision and pattern recognition*, 2016, pp. 770–778. [1](#)
- [15] S. Ren, K. He, R. Girshick, J. Sun, Faster r-cnn: Towards real-time object detection with region proposal networks, in: *Advances in neural information processing systems*, 2015, pp. 91–99. [1](#)
- [16] K. He, G. Gkioxari, P. Dollár, R. Girshick, Mask r-cnn, in: *Proceedings of the IEEE international conference on computer vision*, 2017, pp. 2961–2969. [1](#)
- [17] Y. Srivastava, V. Murali, S. R. Dubey, Hard-mining loss based convolutional neural network for face recognition, *arXiv preprint arXiv:1908.09747*. [1](#)

- [18] S. R. Dubey, S. Chakraborty, Average biased relu based cnn descriptor for improved face retrieval, arXiv preprint arXiv:1804.02051. 1
- [19] H. Li, P. He, S. Wang, A. Rocha, X. Jiang, A. C. Kot, Learning generalized deep feature representation for face anti-spoofing, IEEE Transactions on Information Forensics and Security 13 (10) (2018) 2639–2652. 1
- [20] C. Nagpal, S. R. Dubey, A performance evaluation of convolutional neural networks for face anti spoofing, in: 2019 International Joint Conference on Neural Networks (IJCNN), IEEE, 2019, pp. 1–8. 1
- [21] D. Patel, X. Hong, G. Zhao, Selective deep features for micro-expression recognition, in: 2016 23rd International Conference on Pattern Recognition (ICPR), IEEE, 2016, pp. 2258–2263. 1
- [22] S. P. T. Reddy, S. T. Karri, S. R. Dubey, S. Mukherjee, Spontaneous facial micro-expression recognition using 3d spatiotemporal convolutional neural networks, arXiv preprint arXiv:1904.01390. 1
- [23] W. Zhao, S. Du, Spectral-spatial feature extraction for hyperspectral image classification: A dimension reduction and deep learning approach, IEEE Transactions on Geoscience and Remote Sensing 54 (8) (2016) 4544–4554. 1
- [24] S. K. Roy, G. Krishna, S. R. Dubey, B. B. Chaudhuri, Hybridsn: Exploring 3-d-2-d cnn feature hierarchy for hyperspectral image classification, IEEE Geoscience and Remote Sensing Letters. 1
- [25] P. Isola, J.-Y. Zhu, T. Zhou, A. A. Efros, Image-to-image translation with conditional adversarial networks, in: Proceedings of the IEEE conference on computer vision and pattern recognition, 2017, pp. 1125–1134. 1
- [26] K. B. Kancharagunta, S. R. Dubey, Csgan: Cyclic-synthesized generative adversarial networks for image-to-image transformation, arXiv preprint arXiv:1901.03554. 1
- [27] K. B. Kancharagunta, S. R. Dubey, Cdgan: Cyclic discriminative generative adversarial networks for image-to-image transformation, arXiv preprint arXiv:2001.05489. 1
- [28] K. Sirinukunwattana, S. E. A. Raza, Y.-W. Tsang, D. R. Snead, I. A. Cree, N. M. Rajpoot, Locality sensitive deep learning for detection and classification of nuclei in routine colon cancer histology images, IEEE transactions on medical imaging 35 (5) (2016) 1196–1206. 1, 6
- [29] S. S. Basha, S. Ghosh, K. K. Babu, S. R. Dubey, V. Pulabagari, S. Mukherjee, Rccnet: An efficient convolutional neural network for histological routine colon cancer nuclei classification, in: 2018 15th International Conference on Control, Automation, Robotics and Vision (ICARCV), IEEE, 2018, pp. 1222–1227. 1
- [30] P. e. a. Rajpurkar, Chexnet: Radiologist-level pneumonia detection on chest x-rays with deep learning, arXiv preprint arXiv:1711.05225. 1
- [31] X. Wang, Y. Peng, L. Lu, Z. Lu, R. M. Summers, Tienet: Text-image embedding network for common thorax disease classification and reporting in chest x-rays, in: Proceedings of the IEEE conference on computer vision and pattern recognition, 2018, pp. 9049–9058. 1
- [32] S. R. Dubey, S. K. Roy, S. Chakraborty, S. Mukherjee, B. B. Chaudhuri, Local bit-plane decoded convolutional neural network features for biomedical image retrieval, Neural Computing and Applications (2019) 1–13. 1
- [33] S. Deepak, P. Ameer, Retrieval of brain mri with tumor using contrastive loss based similarity on googlenet encodings, Computers in Biology and Medicine 125 (2020) 103993. 1
- [34] A. Baāzaoui, M. Abderrahim, W. Barhoumi, Dynamic distance learning for joint assessment of visual and semantic similarities within the framework of medical image retrieval, Computers in Biology and Medicine 122 (2020) 103833. 1
- [35] Y. Gu, J. Yang, Densely-connected multi-magnification hashing for histopathological image retrieval, IEEE journal of biomedical and health informatics 23 (4) (2018) 1683–1691. 1
- [36] S. et al., An adversarial learning approach to medical image synthesis for lesion detection, IEEE Journal of Biomedical and Health Informatics. 1
- [37] J. Li, Y. Pu, J. Tang, Q. Zou, F. Guo, Deepvavp: a dual-channel deep neural network for identifying variable-length antiviral peptides, IEEE Journal of Biomedical and Health Informatics. 1
- [38] Q. V. Le, A tutorial on deep learning part 2: Autoencoders, convolutional neural networks and recurrent neural networks, Google Brain (2015) 1–20. 2
- [39] A. Krizhevsky, G. E. Hinton, Using very deep autoencoders for content-based image retrieval., in: ESANN, Vol. 1, 2011, p. 2. 2
- [40] X. Zhang, H. Dou, T. Ju, J. Xu, S. Zhang, Fusing heterogeneous features from stacked sparse autoencoder for histopathological image analysis, IEEE journal of biomedical and health informatics 20 (5) (2015) 1377–1383. 2
- [41] B. Leng, S. Guo, X. Zhang, Z. Xiong, 3d object retrieval with stacked local convolutional autoencoder, Signal Processing 112 (2015) 119–128. 2
- [42] Z. Zhu, X. Wang, S. Bai, C. Yao, X. Bai, Deep learning representation using autoencoder for 3d shape retrieval, Neurocomputing 204 (2016) 41–50. 2
- [43] A. G. Dastider, F. Sadik, S. A. Fattah, An integrated autoencoder-based hybrid cnn-lstm model for covid-19 severity prediction from lung ultrasound, Computers in Biology and Medicine 132 (2021) 104296. 2
- [44] A. Sharma, B. Singh, Ae-lgbm: Sequence-based novel approach to detect interacting protein pairs via ensemble of autoencoder and lightgbm, Computers in Biology and Medicine 125 (2020) 103964. 2
- [45] F. J. Martinez-Murcia, A. Ortiz, J.-M. Gorriz, J. Ramirez, D. Castillo-Barnes, Studying the manifold structure of alzheimer’s disease: A deep learning approach using convolutional autoencoders, IEEE Journal of Biomedical and Health Informatics. 2
- [46] C. Zhou, Y. Jia, M. Motani, Optimizing autoencoders for learning deep representations from health data, IEEE journal of biomedical and health informatics 23 (1) (2018) 103–111. 2
- [47] X. Wang, Y. Shi, K. M. Kitani, Deep supervised hashing with triplet labels, in: Asian conference on computer vision, Springer, 2016, pp. 70–84. 2
- [48] Y. Cao, M. Long, J. Wang, H. Zhu, Q. Wen, Deep quantization network for efficient image retrieval, in: Thirtieth AAAI Conference on Artificial Intelligence, 2016. 2
- [49] Z. Cao, M. Long, J. Wang, P. S. Yu, Hashnet: Deep learning to hash by continuation, in: Proceedings of the IEEE international conference on computer vision, 2017, pp. 5608–5617. 2
- [50] T. Yao, F. Long, T. Mei, Y. Rui, Deep semantic-preserving and ranking-based hashing for image retrieval., in: IJCAI, 2016, pp. 3931–3937. 2
- [51] H. Liu, R. Wang, S. Shan, X. Chen, Deep supervised hashing for fast image retrieval, in: Proceedings of the IEEE conference on computer vision and pattern recognition, 2016, pp. 2064–2072. 2
- [52] H.-F. Yang, K. Lin, C.-S. Chen, Supervised learning of semantics-preserving hash via deep convolutional neural networks, IEEE transactions on pattern analysis and machine intelligence 40 (2) (2017) 437–451. 2
- [53] Q. Li, Z. Sun, R. He, T. Tan, Deep supervised discrete hashing, in: Advances in neural information processing systems, 2017, pp. 2482–2491. 2
- [54] J. Zhang, Y. Peng, Ssdh: semi-supervised deep hashing for large scale image retrieval, IEEE Transactions on Circuits and Systems for Video Technology 29 (1) (2017) 212–225. 2
- [55] Q.-Y. Jiang, W.-J. Li, Asymmetric deep supervised hashing, in: Thirty-Second AAAI Conference on Artificial Intelligence, 2018. 2
- [56] D. Wu, Q. Dai, J. Liu, B. Li, W. Wang, Deep incremental hashing network for efficient image retrieval, in: Proceedings of the IEEE Conference on Computer Vision and Pattern Recognition, 2019, pp. 9069–9077. 2
- [57] J. Wang, Z. Fang, N. Lang, H. Yuan, M.-Y. Su, P. Baldi, A multi-resolution approach for spinal metastasis detection using deep siamese neural networks, Computers in biology and medicine 84 (2017) 137–146. 2
- [58] D. P. Kingma, J. Ba, Adam: A method for stochastic optimization, arXiv preprint arXiv:1412.6980. 4
- [59] S. R. Dubey, S. Chakraborty, S. K. Roy, S. Mukherjee, S. K. Singh, B. B. Chaudhuri, diffgrad: An optimization method for convolutional neural networks, IEEE Transactions on Neural Networks and Learning Systems. 4
- [60] F. Schroff, D. Kalenichenko, J. Philbin, Facenet: A unified embedding for face recognition and clustering, in: Proceedings of the IEEE conference on computer vision and pattern recognition, 2015, pp. 815–823. 6